2024-36-0160

Large-bore HFO Engine Gas Conversion for Power plants – Part A: Numerical Assessment

Vinícius Fernandez Gonçalves, Clayton Barcelos Zabeu, Jácson Antolini
Instituto Mauá de Tecnologia
Guenther Carlos Krieger Filho
Universidade de São Paulo
Roberto Salvador
Linhares Geração
Rogério Almeida, Allan Soares Valiati
Termelétrica Viana

Abstract

In the global scenario marked by the increasing environmental awareness and the necessity on reducing pollutant emission to achieve the decarbonization goals, action plans are being proposed by policy makers to reduce the impact of the climate change, mainly affecting the sectors that most contribute to CO2 emissions such as transportation and power generation. In this sense, by virtue of the National Energy Plan 2050, the Brazilian market will undergo the decommissioning of thermal power plants fueled by diesel and heavy fuel oil (HFO) by 2030, compromising about 6.7 GW of power capacity according to the Brazilian Electricity Regulatory Agency (ANEEL) database. An alternative to the scrapping of these engine power plants is their conversion to operate with fuels with a lower carbon footprint, such as the natural gas. This work, therefore, aims to numerically assess the conversion feasibility of a HFO large bore four-stroke turbocharged engine to operate with natural gas by means of a one-dimensional engine modeling. First, the 1D non-converted engine model operating with HFO is validated with experimental data. Then, the conversion of the HFO engine to natural gas is carried out by adding a wastegate for the air-fuel ratio control, changing the compression ratio and the fuel injection, and introducing the pre-chamber ignition system. At this stage, the performance of the engine operating with most of its stock components is evaluated, including the presence of knock, fuel slip, and components that may not be suitable for NG operation and must be adapted, redesigned, or replaced. After that, modifications on the valve timings are proposed to reduce the methane slip and allows a proper scavenging. In conclusion, this study numerically assessed converting an HFO engine to natural gas, identifying new component specifications and presenting alternatives to maintain engine performance post-conversion.

Introduction

Over the past few decades, the world's need for energy has increased, either as a result of population expansion or national economic progress [1]. Fossil fuels, including coal, oil, and natural gas, are the primary sources of energy supply worldwide and are recognized to be major contributors of greenhouse gas emissions [2]. Although it has been rising over the past years, the share of renewable energy sources—such as hydropower, wind, solar power, biofuels, etc.—remains small in comparison to more polluting sources like coal and heavy oil.

It is commonly acknowledged that human activity contributes to greenhouse gas emissions, and that there is a connection between CO2 emissions and the increase in global temperatures [3]. When compared to the half-century between 1850 and 1900, the global surface temperature has risen by 1.1 ºC in the previous ten years, which correlates with both the concentration and emission of greenhouse gases due to human activity [4]. Thus, the primary cause of the global warming can be attributed to the CO2 emissions from the burning of fossil fuels to generate energy or power the transportation industry [5].

In the context of power generation, subject of this work, thermoelectric power plants operating with an internal combustion engine (ICE) play an important role in the energy matrix to ensure a stable and reliable grid during peak consumption periods or when the hydroelectric reservoir levels are low or the sunshine and wind are not available. The thermoelectric power plants are capable to provide a fast start-up time, flexible output range (by connecting multiple ICE units) without compromising efficiency, and excellent ramp load rate. Such characteristics make it a good option for balancing variations over the day and between seasons on electric power systems.

In this sense, due to the current dependency on fossil fuels and the high financial and temporal cost of moving to a greener energy matrix, improving the efficiency of the current fossil-based thermal power plants without significantly raising their short- to medium-term purchase and operating costs is a necessary and intermediate step to reduce greenhouse gas emissions.

According to the 2023 Brazilian Electrical Energy Statistical Yearbook [6], the installed capacity of thermal power plants corresponds to 21.4% of the 206.5 GW available in Brazil, and the energy actually generated by those using fuel oil represented only 1.2% of the total (7816 GWh) in 2023. Compared to 2022, there was a decrease of about 57% for thermal power plants fueled by petroleum derivatives, indicating a significant decline in electricity

generation from these sources as a result of a great availability of renewable sources.

Given economic and environmental factors, the Brazilian National Energy Plan 2050 [7] determine the decommissioning of thermal power plants fueled by diesel and heavy fuel oil (HFO) by 2030, which corresponds to 6,7 GW of the installed capacity [8]. In light of this decommissioning, there are two options for the hundreds of engines currently powered by HFO in Brazil: (1) scrapping or (2) converting to a fuel with a lower carbon footprint. The cost of a "full" conversion process, however, can reach up to 80% of a new engine when carried out by the manufacturer, harming the competitiveness of the power plant in relation to other sources. The full conversion process aims to maintain the engine brake power at the expense of increasing its displaced volume and the replacement of high-cost components such as the turbochargers and pistons.

An alternative to a full engine conversion is a conversion using most parts from the base engine, reducing the cost of transportation and importation to Brazil, with some penalty on the brake power and efficiency as a consequence of the reuse of parts that are not optimal for operation with natural gas. This work aims to numerically assess the performance, the fuel conversion efficiency, and the limitations arising from a conversion of a large-bore HFO engine to operate with natural gas, as well as the possible paths of efficiency improvement while avoiding fuel slip to the exhaust system. Furthermore, the numerical model will support the decision making to the conversion of 1 of the 20 cylinders in the Tevisa power plant (Figure 1) by providing important information for manufacturing prototype components.

Figure 1. Engine generators at the power plant Tevisa located at Espírito Santo powered only by heavy fuel oil.

First, the numerical tools used in this numerical assessment are described. Then, the HFO engine model is created and validated with experimental results for both full and partial loads. After that, the numerical model is modified to operate with natural gas with minor modifications on the engine, and the numerical results are presented and discussed, highlighting the main drawbacks. Next, a parametric study is carried out to find an optimum valve timing considering the existing camshaft with minor modifications on the lobes. Finally, the main outcomes are summarized in the conclusions.

This work is supported by a group of power plants, Tevisa, Linhares, Tropicália, and Povoação, as part of a research and development project regulated by the Brazilian National Electric Energy Agency (ANEEL).

Methods

Baseline Engine

The engine target for this conversion project (Wartsila W20V32) is a turbocharged four-stroke large-bore engine widely used in thermal power plants or vessels. The 20 cylinders are distributed in a V configuration between banks A and B. The fuel (HFO or diesel) is direct injected into the combustion chamber. The cylinder bore is 320 mm with a stroke of 400 mm, resulting in a displacement volume of 32.2 liters per cylinder. The brake power at full load is 9000 kW (450 kW per cylinder), operating at a fixed speed of 720 rpm to achieve 60 Hz in the electrical power grid. Table 1 displays some technical specifications of this engine.

Table 1. Technical data of the Wartsila W20V32 engine.

Technical Specifications Wartsila W20V32 (full load)		
Engine Speed	720	rpm
Number of cylinders	20	-
Number of valves per cylinder	2 intake and 2 exhaust	-
Brake Power	9000	kW
BMEP	23,3	bar
IMEP	25,2	bar
Bore	320	mm
Stroke	400	mm
Connecting Rod Length	848	mm
Clearance height at TDC	10,68	mm
Compression Ratio	16:1	-

Numerical Simulations

The numerical simulations were conducted using the GT-Power software from Gamma Technologies. The GT-Power is one of the tools available in the GT-Suite library and is focused to 1D simulation of propulsion systems. It is widely used in the automotive industry to simulate internal combustion engines, where many components can be modeled with advanced concepts [9–11]. This software features a highly versatile graphical interface, called GT-ISE (Integrated Simulation Environment), which is used in all its applications, simplifying the tasks of managing libraries, building, editing, executing, and post-processing models [12].

To understand how the GT-Power works a brief description is presented: the code is based on one-dimensional fluid dynamics, representing the flow and heat transfer in the piping and other engine components. The model involves solving the Navier-Stokes equations, which include the continuity, momentum, and energy equations, and these are solved only in the direction of the flow (1D)

[13]. The Navier-Stokes equations are shown in equation 1, 2, 3 and 4.

$$\frac{dm}{dt} = \sum_{boundaries} (\dot{m}) \quad (1)$$

$$\frac{d(me)}{dt} = -\frac{\rho dV}{dt} + \sum_{boundaries} (\dot{m}H) - hA_s(T_{fluid} - T_{wall}) \quad (2)$$

$$\frac{d(\rho HV)}{dt} = \sum_{boundaries} (\dot{m}H) + \frac{Vdp}{dt} - hA_s(T_{fluid} - T_{wall}) \quad (3)$$

$$\frac{d\dot{m}}{dt} = \frac{dpA + \sum_{boundaries}(\dot{m}u) - 4C_f \frac{\rho u|u|}{2}\frac{dxA}{D} - K_p\left(\frac{1}{2}\rho u|u|\right)}{dx} \quad (4)$$

Where $\dot{m}$ is the mass flow rate at the boundary of the volume, m is the mass, V is the volume, p is the pressure, ρ is the density, A is the cross-sectional flow area, A_s is the heat transfer surface area, e is the specific internal energy, H is the specific absolute energy, h is the heat transfer coefficient, T_{fluid} is the fluid temperature, T_{wall} is the wall temperature, u is the velocity at the boundary, C_f is the friction factor, K_p is the loss coefficient, D is the equivalent diameter, dx is the element length in the flow direction and dp is the pressure difference along dx.

The system is discretized into several volumes, where each part of the flow is represented by a single volume, and each pipe is divided into one or more volumes that are connected by boundaries. Within these volumes, scalar variables (pressure, temperature, specific mass, enthalpy, species concentration, etc.) are considered uniform. Vector variables (velocity, mass flow rate, etc.) are calculated for each boundary.

In this work, these simulations will be responsible for numerically calculate the engine efficiency, brake power, fuel consumption, pressures, and mass flows of the engine at partial and full loads. In the case of the HFO engine, the experimental data will be compared with the simulation to prove the validity of the model. After that, the engine model will be converted to operate with NG to evaluate the performance of the engine with most of its stock components.

W20V32 HFO Engine

One of the first steps in performing the modeling is to specify the engine's technical data. Initially, the characteristics of the engine, such as bore, stroke, and compression ratio, were added, which can be found in Table 1.

The diagrams for the intake and exhaust valves, as well as the discharge coefficients of these valves, were incorporated into the model. Figure 3 displays the valve lift of the W32. The discharge coefficients were derived from a previously validated model of the W34SG, which shares the same ports and valves geometries as the W32 version.

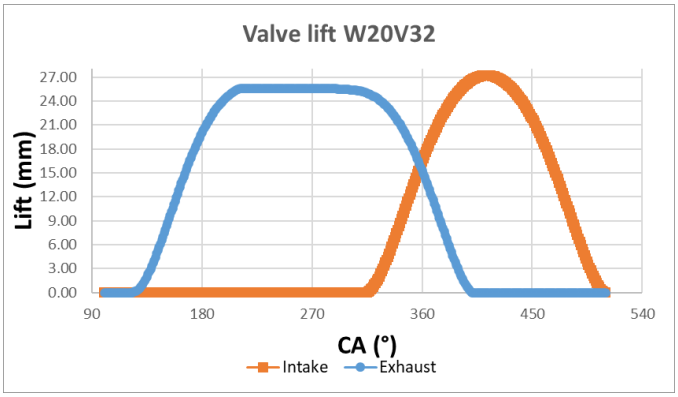

Figure 3. Valve lift W20V32.

The implemented direct injection system works according to the setpoint of the engine power, adjusting the amount of fuel injected into the cylinder depending on the target load. The fuel used is diesel and its characteristics are available in GT-Power library. The lower heating value of the fuel, however, was changed to be compatible with the experimental data.

In the next sub-sections, the main components that have been modeled are described and its control strategy is presented. Figure 2 shows a panoramic view of the engine model containing all components divided into blocks

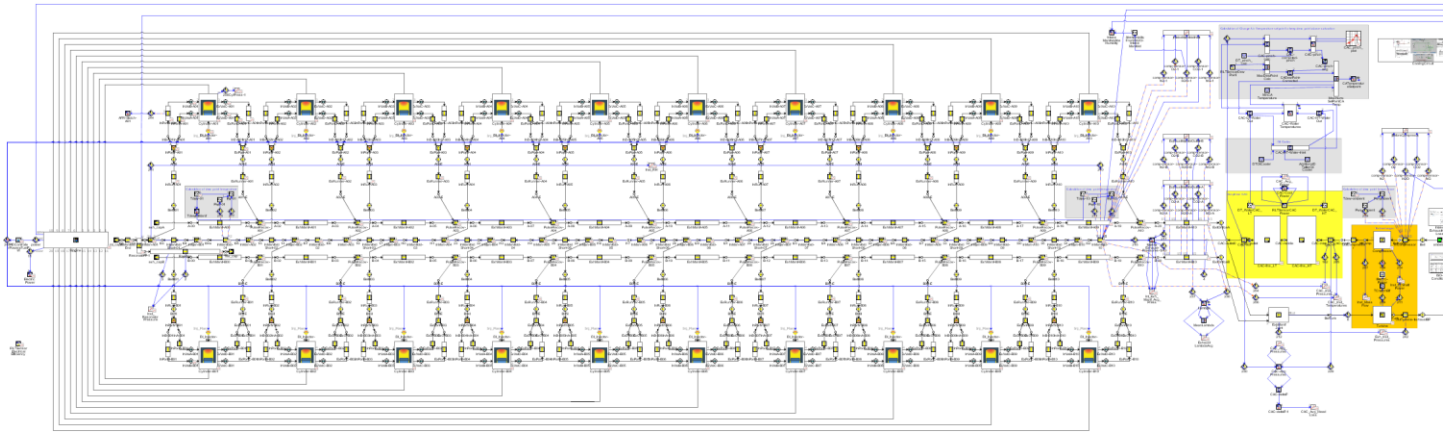

Figure 2. GT-Power 1D model.

Turbochargers

The first component to be addressed is the turbocharger, where the work generated by the enthalpy of the exhaust gases is utilized to compress the intake air. The intake air of the engine follows a path from the air filter housing to the inlet of the compressor.

The W20V32 engine configuration employs two turbochargers, each one responsible for 10 engine cylinders or one bank. To setup this component in the absence of efficiency maps, the equivalent diameter of the turbine and the efficiencies of both turbine and compressor were adjusted to match the intake and exhaust pressures according to its load.

Charge air coolers

The charge air coolers (CAC) aim to reduce the intake air temperature after the compressor. The baseline engine has two intercoolers: the high-temperature (HT) CAC and the low-temperature (LT) CAC. At the compressor outlet, the air is first conducted to the HT CAC and then to the LT CAC, reducing the air temperature to a specified value according to the operating strategy. The CACs exchange heat with the engine coolant, which first is cooled on the radiators and then conducted to the LT CAC. Next passes through the engine lubricant heat exchanger, and then is conducted to the HT CAC. Finally, the coolant is directed to cool the engine.

During the engine operation, the intake air temperature setpoint after the CAC is defined by the dew point temperature to prevent the water condensation. Therefore, the engine cooling strategy calculate the dew point in the intake manifold and establishes a 2°C safety margin from it, maintaining the temperature close to this value by controlling the opening of the three-way thermostat valves and the frequency of the radiator fans. Basically, the dew point temperature at the intake manifold is in function of the ambient conditions, such as temperature, pressure, and humidity of the air. This control strategy is implemented in the engine model, and it is responsible for determining the air temperature at the outlet of the CACs. Regarding the air flow in the CACs, the losses coefficients are also considered for each CAC, resulting in a corresponding pressure drop.

Burn rate

The combustion profile of the W32 engine was also calculated using the GT-Power. The approach used in this model is called Cylinder Pressure Only Analysis (CPOA), which is described in the following [12]:

1. At beginning of a cycle, a rough calculation of combustion burn rate is done making some assumptions about heat transfer (Woschni).
2. The resulting burn rate is applied during the forward simulation cycle and the true heat transfer rate is stored.
3. A final burn rate calculation is done with the true heat transfer from the simulation and all results stored.
4. The final burn rate is applied during the forward simulation cycle in order to provide a comparison of measurement versus simulation.

The burn rate GT-Power model is shown in Figure 4. It is a simple model, where the main input data are geometric characteristics of an engine cylinder (such as bore, stroke, compression ratio), the heat transfer model, the instantaneous in-cylinder pressure curve as a function of the crankshaft angle, the volumetric efficiency, and the percentage of residual gas in the cylinder. The average pressure curve of the 20 cylinders for 30 cycles at full load is presented in Figure 5.

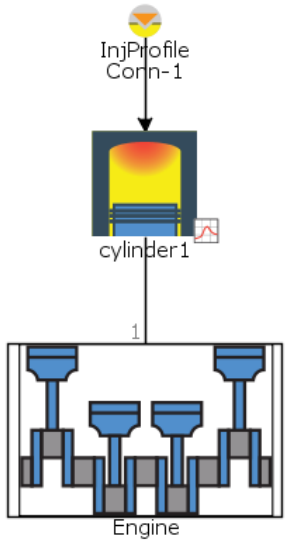

Figure 4. Burn rate model.

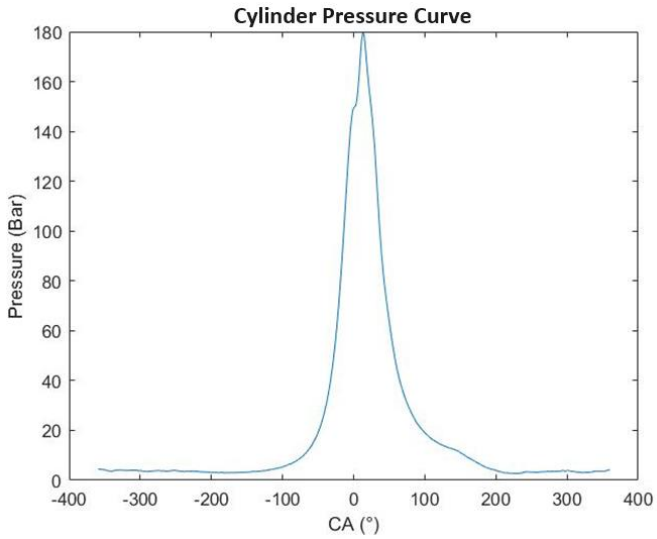

Figure 5. Measured cylinder pressure curve.

With all these data, it was possible to generate the simulated burn rate profile of the W20V32 at full load, which is imposed in the HFO engine model. The result is shown in Figure 6.

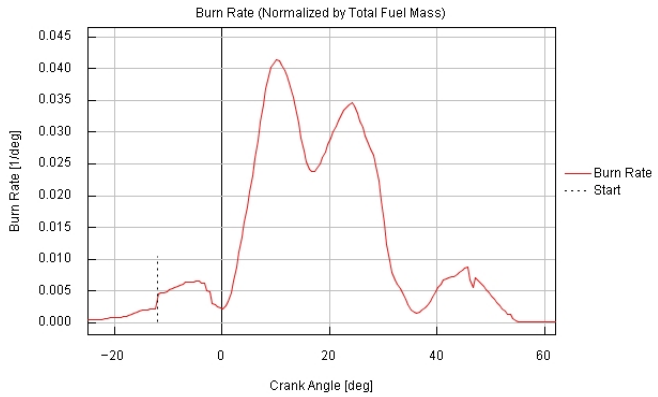

Figure 6. Burn rate HFO using GT-Power simulation.

W20V32SG Gas Engine

The conversion process proposed in this project aims to use most of the components from the original HFO engine. Therefore, the model developed at this stage of the W20V32SG (designation given to the machine converted from HFO to NG) aims to evaluate the performance of the generator set with its original parts and analyze the components that will not be compatible and need to be adapted, redesigned, or replaced.

Due to unavailability of experimental data of the W20V32 engine operating with NG, some assumptions were considered using both experimental and numerical data of the Wartsila NG engine W20V34SG. Similar to the HFO version, the W20V34SG is a 20-cylinder V-architecture engine with 4 valves per cylinders. The differences, however, relies on the larger cylinder bore (340mm), and the PFI NG injection associated with an active pre-chamber ignition system, producing a brake power of 8700 kW (435 kW per cylinder) at 720 rpm.

A description regarding the engine's modifications needed to operate with NG is approached in this section.

Compression ratio

In order to avoid knock limitation, the compression ratio must be reduced. For this purpose, there are two solutions already provided by Wartsila that will be adopted. The first is the use of a shim placed between the engine block and the cylinder liner seat, thereby increasing the dead volume of the combustion chamber and consequently reducing the compression ratio. The second solution involves replacing the connecting rod shim with a thinner one to reduce the total length (and consequently the dead volume), resulting in a lower compression ratio. With both shims installed, the estimated compression ratio is 13.9:1.

Wastegate

To adjust the air/fuel ratio, a wastegate was implemented in the simulation. Its control is carried out by opening or closing the valve according to the 20 cylinders averaged combustion lambda at EVO. For each cycle, the control strategy adopted by the software reduce or increase the valve passage area to reach the target lambda.

Injection system

For the injection system, it was necessary to include the active prechamber and the PFI gas injector in the simulation. Similar to the HFO version, the amount of gas injected is adjusted according to the power target. The fuel is injected at the port and in the prechamber during the intake stroke. Due to the large valve overlap, studies had to be conducted to prevent fuel slip into the exhaust system and to allow enough time for the fuel to enter the cylinder. This involved determining the correct injection timing and fuel mass flow of the injector, by controlling the supply gas pressure of the SOGAV. Figure 7 illustrates a comparison between the optimized injection system of the W32SG and W34SG engines for the mass fraction of NG at both exhaust ports. As depicted, at the exhaust ports, the W32SG exhibits less fuel slip than the W34SG. It is worth noting that the valve overlap of the W34SG is significantly small compared to W32. These mass fractions pertain to the most critical cylinder, which is the A01.

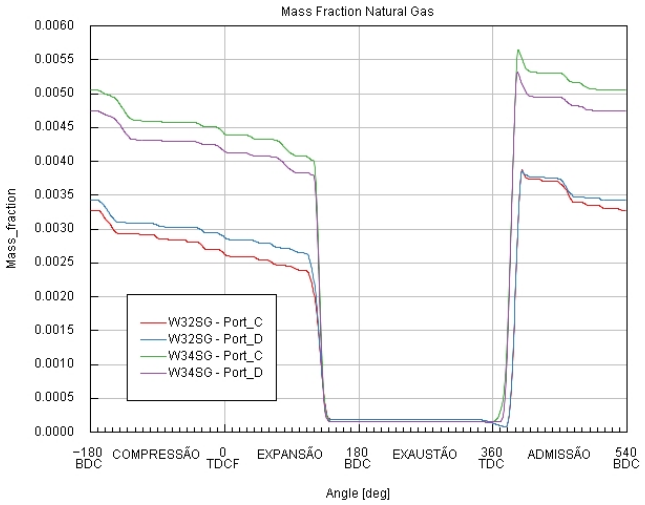

Figure 7. Mass Fraction of NG at the exhaust ports in the W32SG and W34SG.

Burn rate

At this stage, given the unavailability of experimental data for the converted NG engine, the burn rate is assumed to be the same as the Wartsila W34SG engine, experimentally obtained in previous works [14]. The authors are aware that differences between the W34SG and the W32SG burn rate may arise due to differences in the piston and combustion chamber geometries, but any potential deviation will be addressed as soon as the experimental data of the converted W32SG engine are available. The normalized burn rate of the W34SG engine at full load is shown in Figure 8.

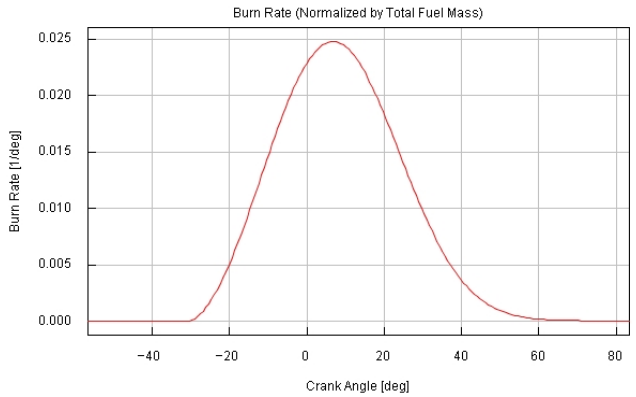

Figure 8. Normalized burn rate of the W34SG engine at full load.

Results and Discussion

In this section, the validation of the HFO engine and the results related to the NG converted engine is shown.

HFO Results

The HFO experiments data was obtained, for the following operating conditions: at 60%, 85% and 100% of load at 720 rpm. For these points the magnitudes of brake power, intake pressure, intake and exhaust temperatures are measured in the engine. The BSFC is only available at full load. With these experimental and simulated results, it was possible to evaluate the reliability of the model.

Figure 9 and Figure 10 shows the brake power curve and absolute intake pressure. As indicated, the experimental and simulation results for the three operational points follows the engine curve. Deviations of less than 1% is seen in these results.

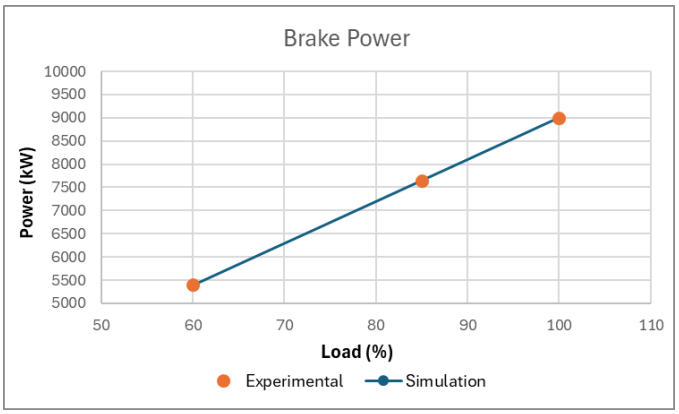

Figure 9. Brake power curve.

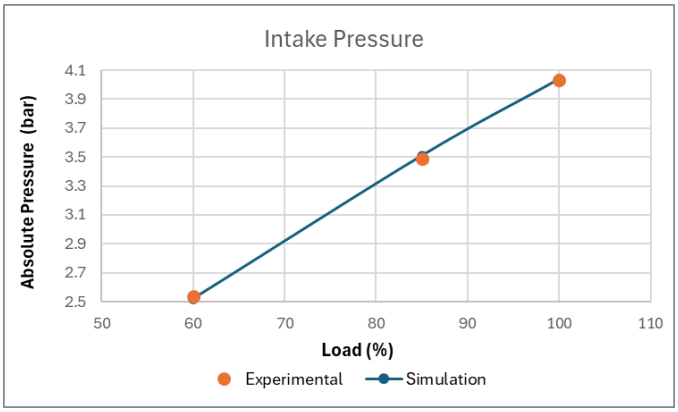

Figure 10. Intake pressure curve.

The air temperature in the CAC and the average exhaust temperatures are displayed in Figure 11 and Figure 12. The maximum difference temperature observed in the outlet of the CAC for the three operational points is less than 3°C. These results demonstrate the validity of the CAC model. For the exhaust temperatures, the major difference is found at full load, with a deviation of 18°C and 12°C for Bank A and B, respectively.

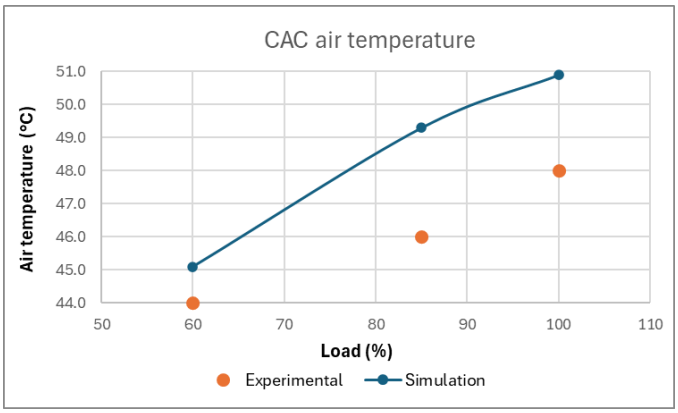

Figure 11. CAC air temperature curve.

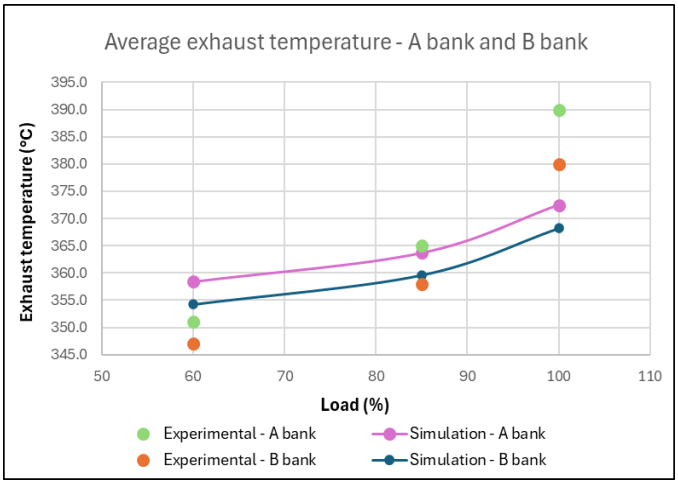

Figure 12. Average exhaust temperature at A and B bank.

The cylinder pressure curve was also evaluated in Figure 13. The red curve represents the simulated curve, and the blue one represents the experimental curve. It was possible to observe that there is a significant difference both during the expansion cycle and the exhaust cycle. The pressures in the intake and compression are as expected. Given this, it was necessary to investigate the cause of this discrepancy between the graphs. Therefore, it was decided to conduct a case study to analyze the impact of pressure measurement using the rubinet. In the W20V32 engine, pressure is measured using a tool that is installed only during verification. This tool is a tube, called rubinet, with approximately 6 mm in diameter and 400 mm in length, which has some curves along its path inside the cylinder head. A piezoresistive pressure sensor is installed at the end of this tube. This method introduces an oscillation due to the resonance frequency in the tube and, therefore, is not the most appropriate for this purpose. This study was important to understand the behavior of the pressure curve.

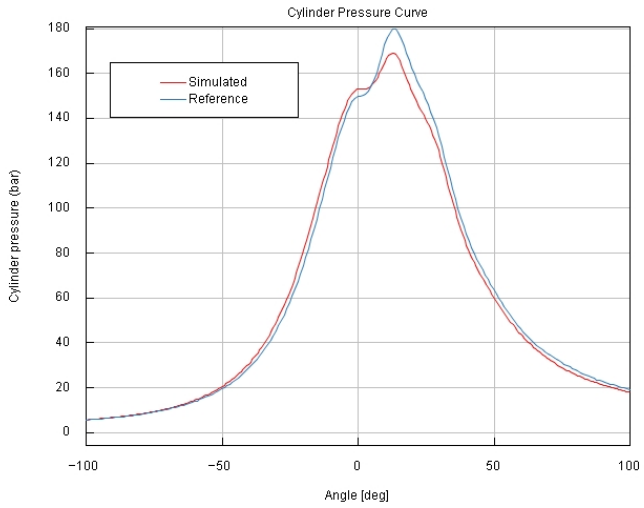

Figure 13. Experimental and simulated cylinder pressure curve.

A final verification was the addition of the rubinet tube in the simulation to try to visualize how the pressure in the cylinder is influenced by this. Figure 14 show this comparison with the three pressure curves: simulated (red), experimental (blue), and simulated with the rubinet (green). In this specific case with the rubinet, a slight delay is observed compared to the other curves, a peak pressure consistent with the experimental data, and a resonance frequency from the tube. Therefore, based on this result, the new curve obtained seems to be adequate compared to the already filtered experimental curve (blue).

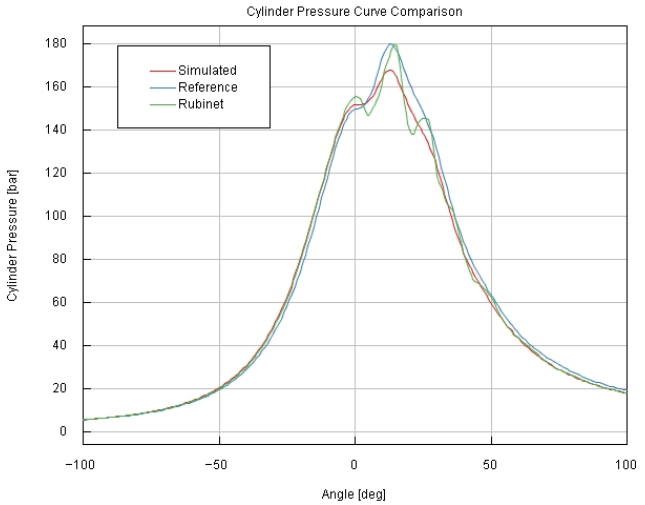

Figure 14. Experimental, simulated and rubinet simulated cylinder pressure curve.

NG Engine Conversion

Through this simulation, it was possible to evaluate the power of the complete engine generator (20 cylinders) running on natural gas. The strategy used to operate the engine at full load was to adjust the fuel control system, ensuring the engine reaches lambda 2 with the wastegate completely closed (similar to the W20V34SG engine). This directs the exhaust gases directly to the turbine, in other words, without the bypass (wastegate), to utilize the exhaust gas enthalpy and generate more work in the compressor, ensuring a higher air flow in the intake. By default, the amount of fuel is defined by the engine load, and the air-fuel ratio is adjusted by controlling the effective passage area of the wastegate. As expected, at full load, there was a drop of 1 MW in the machine's power, resulting in 7960 kW of brake power (20.62 bar – BMEP) and a maximum lambda of 1.9. It is important to note that this result is based on the adopted hypotheses previously reported.

A second finding from the simulation is the inability to reach lambda 2. This characteristic was attributed to the valve timing, where this component shows a large valve overlap (Figure 3) compared to the natural gas engine. This means that the amount of air admitted by the engine is not sufficient to maintain a lambda ratio of 2, requiring a change in the valve timing diagram or even the turbocharger to allow a higher air flow. Another point observed regarding the valve timing is the difference between the lambda measured at the exhaust and the effective combustion lambda. When reading the lambda at full load in the exhaust, the value is around 2.2, while in the cylinder, the effective lambda is 1.9. This is another characteristic of the large valve overlap, where the intake air passes directly to the exhaust during that period, making the measured lambda in the exhaust region leaner.

Based on this study of the valve timing, it was decided to modify the valve timing to reduce the overlap. As consequence this also helps to prevent the slipping of natural gas from the intake to the exhaust system [15].

New simulations had to be performed to create a new intake and exhaust lift profiles. The method used was at a fixed BMEP of 20 bar and wastegate totally closed, analyzing the combustion lambda,

trapping ratio, residual gas, intake pressure, power, and efficiency of the engine to determine a new intake and exhaust profile. The new camshaft was simulated using the following approach:

1. Reducing the closing ramp of the exhaust and the opening ramp of the intake by 1° for each case. This means both profiles will be adjusted to close (exhaust) and open (intake) 1° earlier in each simulation, leading to progressively smaller valve timing.
2. Reducing the exhaust timing by 1° per simulation while shifting the set to the correct TDC.

A point to highlight is that the up and down ramp of the command will be maintained to result in the already known dynamic forces and not impact the valvetrain.

According to Figure 15, the simulations using the first approach resulted in a decrease in combustion lambda rather than an increase. This can be explained by the reduction in intake timing, which leads to a reduced air mass available in the cylinder, decreasing the lambda for the given BMEP. However, it is important to note that the engine efficiency increased due to the reduction in overlap. The exhaust temperatures also changed due to the short-circuit, which results in fresh air entering in the exhaust system. Additionally, the difference between combustion and exhaust lambda also decreased.

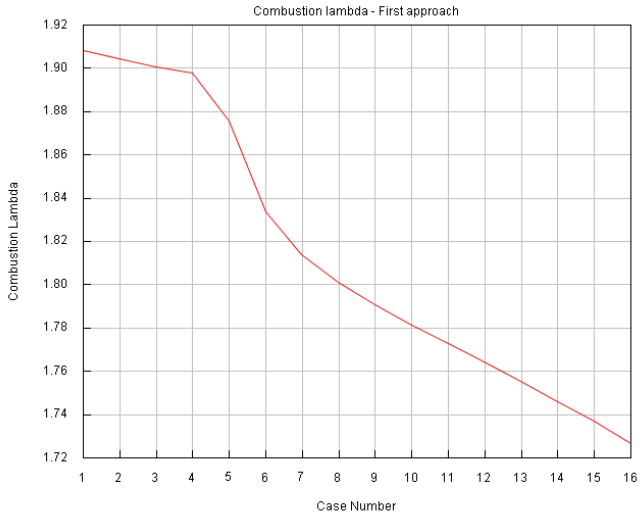

Figure 15. Average combustion lambda using the first approach. The first case refers to the standard camshaft without modifications.

The second approach, which involved reducing only the exhaust timing and adjusting the set, brought satisfactory results. As shown in Figure 16, the combustion lambda increased with this method, reaching the target of lambda 2.

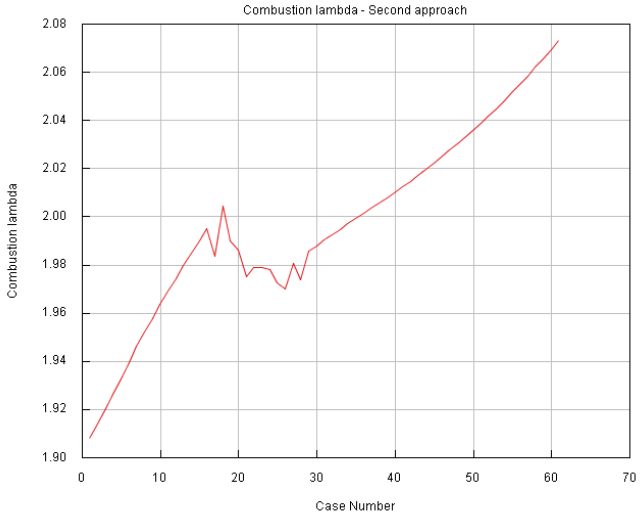

Figure 16 – Average combustion lambda using the second approach.

The brake efficiency is presented in Figure 17. Reducing the valve overlap results in an increase in brake efficiency. However, after case number 40, the efficiency begins to drop. This is due to an increase in lambda, which changes the simulation burn rate profile, causing slower combustion and impacting the studied parameters.

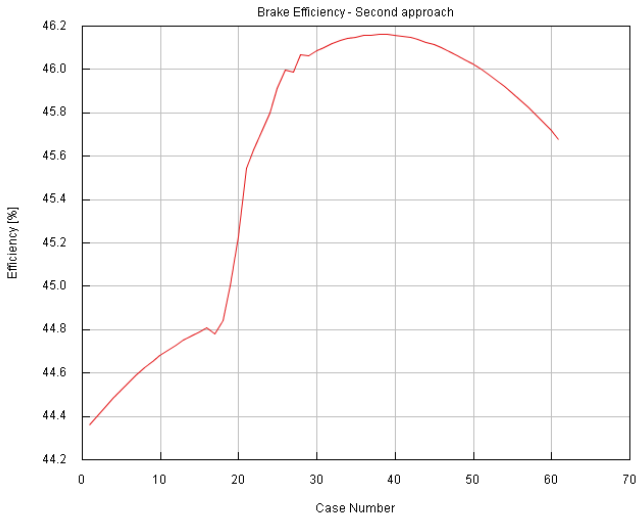

Figure 17 – Brake efficiency using the second approach.

Figure 18 shows the volumetric efficiency. This parameter decreased when reducing the valve overlap. The enthalpy of the exhaust gases became lower, which affected the work of the turbine and compressor, reducing the volumetric efficiency.

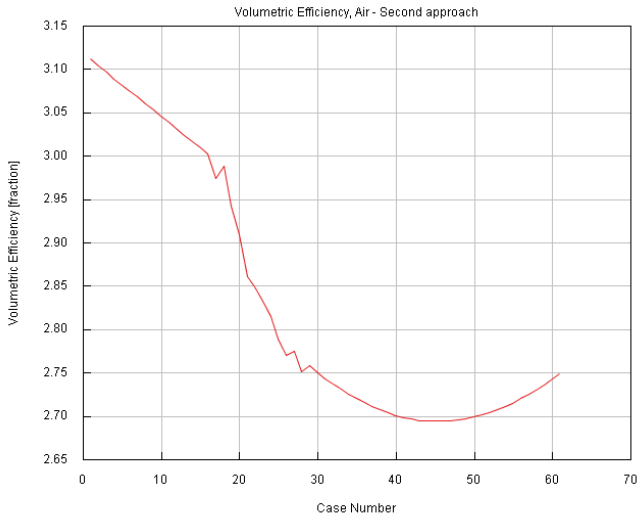

Figure 18 – Volumetric efficiency using the second approach.

The trapping ratio in Figure 19 exhibits the same behavior as the other two graphs. With a reduced short-circuit effect in the cylinder, the trapping ratio inside the cylinder is higher.

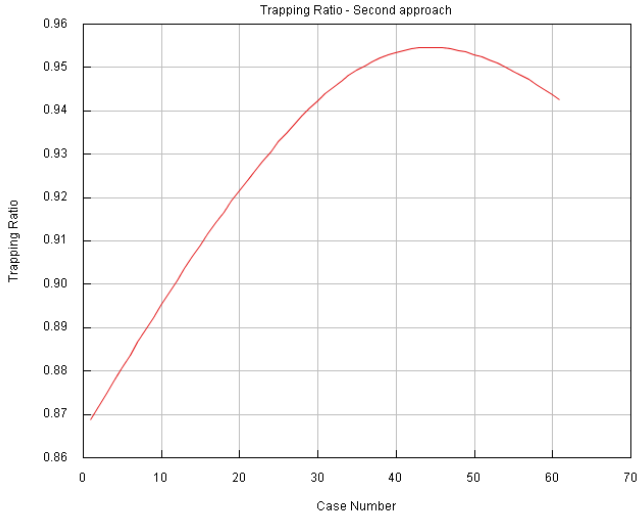

Figure 19 – Trapping ratio using the second approach.

According to Figure 20, reducing the exhaust valve timing tends to increase the residual gas in the cylinder. It is worth noting that even with the smaller valve overlap simulated for the W32, the residual gas percentage was lower than that of the NG Wartsila engine version.

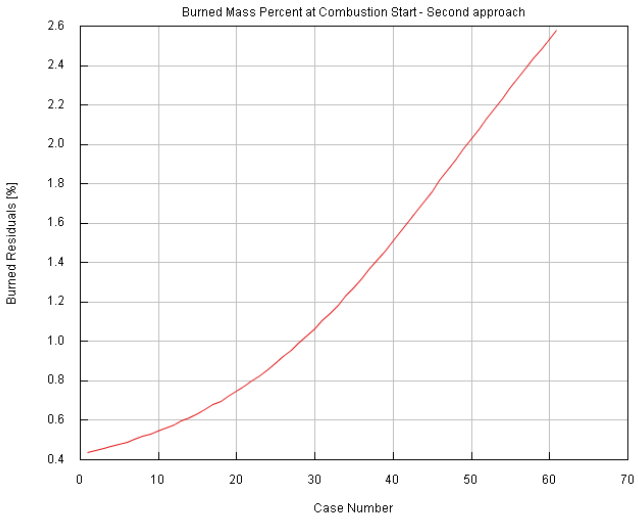

Figure 20 – Residual Gas using the second approach.

Based on these results, it was possible to develop an optimized camshaft for NG. To achieve the best scenario with a focus on cost-effectiveness, avoiding major modifications for machining and reaching the target lambda, the chosen approach involves reducing the exhaust timing by 60° and shifting the set by 30° to align with TDC. Figure 21 shows the modified valve lifts for NG.

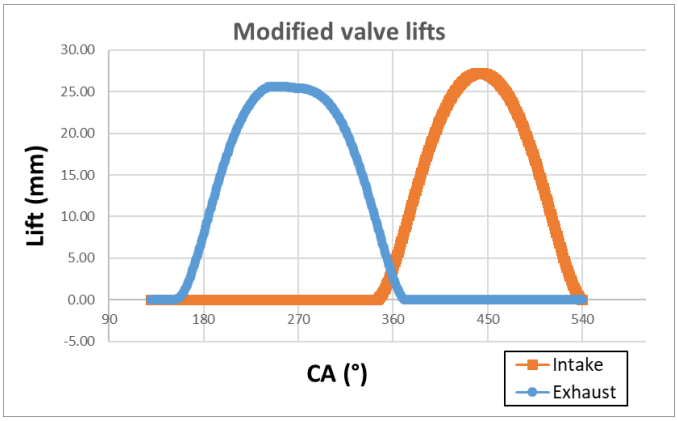

Figure 21 – Modified camshaft.

Table 2 shows a comparison of some results obtained for the standard camshaft and the optimized version at full load.

Table 2. Numerical and experimental results of the W20V32 model at full load.

Full load	Standard	Optimized
Power (kW)	7960.90	9321.44
BMEP (bar)	20.62	24.15
Average combustion lambda	1.90	2.0
Absolute charge air pressure (bar)	3.63	3.78
Charge air temperature in air receiver (°C)	49.5	49.7
Exhaust gas temperature A-bank - mean value (°C)	357.3	423.7
Exhaust gas temperature B-bank - mean value (°C)	353.0	421.6
Efficiency (%)	44.35	46.11
Residual gas (%)	0.45	2.56

Despite the results presented, it is likely that the optimized version will have knock limitation that will affect its performance. Through future experimental tests, these limitations can be addressed, allowing for a more accurate estimation of the converted engine's real performance. Another consideration is that the new camshaft does not feature early intake closing (Miller cycle), which means that the temperatures inside the cylinder will be higher, impacting also with knock. One solution to mitigate the temperature problem is to replace the CAC to one with a larger surface area, resulting in increased heat transfer rate to further cool down the intake air.

Conclusions

This work presented a numerical assessment using GT-Power for the validation of the W20V32 HFO engine and the study of the NG conversion process of the engine. The HFO model demonstrated consistent results at both partial and full load when compared to the experimental data. The deviations were minimal indicating the model's high reliability. Comparing the cylinder pressure curves was useful to understand the pressure behavior inside the cylinder and in the rubinet, in order to evaluate the differences in the obtained results. Regarding the W20V32SG, this study aimed at developing a conversion process using most of the stock components from the HFO version revealed that new components must be redesigned or replaced. The optimized injection system, developed to prevent fuel slip, and the new camshaft design to achieve lambda 2, were obtained from the numerical results based on previous premises. The final performance of the NG engine indicated a significant improvement after modification, with increased power and efficiency. This NG conversion process study will be validated once the experimental data from the converted engine is available.

Acknowledgments

The authors would like to thank Termelétrica Viana S.A. (TEVISA), Linhares Geração S.A. (LGSA), Povoação Energia S.A.(POESA) and Tropicália Transmissora de Energia (TTE) for sponsoring the R&D ANEEL PD-06483-0223/2023 Project.

References

[1] Energy Institute. Statistical Review of World Energy 2023 2023;70:8–20.

[2] International Energy Agency. Energy Statistics Data Browser 2023. https://www.iea.org/data-and-statistics/data-tools/energy-statistics-data-browser.

[3] Lacis AA, Schmidt GA, Rind D, Ruedy RA. Atmospheric CO 2 : Principal Control Knob Governing Earth's Temperature. Science (80-) 2010;330:356–9. https://doi.org/10.1126/science.1190653.

[4] Calvin K, Dasgupta D, Krinner G, Mukherji A, Thorne PW, Trisos C, et al. IPCC, 2023: Climate Change 2023: Synthesis Report. Contribution of Working Groups I, II and III to the Sixth Assessment Report of the Intergovernmental Panel on Climate Change [Core Writing Team, H. Lee and J. Romero (eds.)]. IPCC, Geneva, Switzerland. 2023. https://doi.org/10.59327/IPCC/AR6-9789291691647.

[5] Intergovernmental Panel on Climate Change (IPCC). Climate Change 2022 - Mitigation of Climate Change. Cambridge University Press; 2023. https://doi.org/10.1017/9781009157926.

[6] Empresa de Pesquisa Energética. Anuário Estatístico De Energia Elétrica 2023 2023:1–6.

[7] Ministério de Minas e Energia. PLANO NACIONAL DE ENERGIA 2050 2020:1–232.

[8] Agência Nacional de Energia Elétrica. Sistema de Informações de Geração da ANEEL n.d. https://app.powerbi.com/view?r=eyJrIjoiNjc4OGYyYjQtYWM2ZC00YjllLWJlYmEtYzdkNTQ1MTc1NjM2IiwidCI6IjQwZDZmOWI4LWVjYTctNDZhMi05MmQ0LWVhNGU5YzAxNzBlMSIsImMiOjR9.

[9] Silva Assis MS, De Castro DH, Araújo Moreira TA, Rodrigues Filho FA, Teixeira Malaquias AC, Coelho Baêta JG. Numerical study of compression ratio influence on specific fuel consumption of an ethanol fueled engine using GT POWER code. SAE Tech Pap 2021. https://doi.org/10.4271/2022-36-0075.

[10] Magalhães Avelar FT, de Souza JLF, Rodrigues Filho FA, da Costa RB, Duarte VF, Magalhães Avelar IT, et al. NUMERICAL MODEL OF SI ENGINE USING GT-POWER CODE. SAE Tech. Pap., 2020, p. 1–9. https://doi.org/10.4271/2019-36-0170.

[11] Jadhav V, Kanchan S, Thipse S, Kavathekar K, Dsouza A, Sonawane S. Optimizing and Validating the Engine

Performance and Emission Parameters on Engine Dynamometer through 1D Simulation of a Multi-Cylinder CNG Engine. SAE Tech Pap 2016;2016-Febru. https://doi.org/10.4271/2016-28-0102.

[12] Technologies G. Engine Performance Application Manual 2021.

[13] Technologies G. Flow Theory Manual 2021.

[14] Chun A, Donatelli JLM, Santos JJCS, Zabeu CB, Carvalho M. Superstructure optimization of absorption chillers integrated with a large internal combustion engine for waste heat recovery and repowering applications: Thermodynamic and economic assessments. Energy 2023;263:125970. https://doi.org/10.1016/j.energy.2022.125970.

[15] Yang B, Keller P. Analysis of diesel engine emissions reduction by late intake valve close and VTG turbocharger using 1-D simulation. SAE Tech Pap 2008. https://doi.org/10.4271/2008-01-2444.

Contact Information

Instituto Mauá de Tecnologia - IMT

Vinícius Fernandez Gonçalves:

vinicius.goncalves@maua.br

Definitions/Abbreviations

HFO	Heavy fuel oil
NG	Natural gas
PFI	Port fuel injection
CA	Crankshaft angle
CAC	Charge air cooler
HT	High temperature
LT	Low temperature
CPOA	Closed volume analysis
EVO	Exhaust valve open
SOGAV	Solenoid operated gas valve
RPM	Revolution per Minute
BSFC	Brake specific fuel consumption
TDC	Top dead center
BDC	Bottom dead center
ICE	Internal Combustion Engine

ISSN 0148-7191